Korean J. Chem. Eng., 35(3), 798-804 (2018)
DOI: 10.1007/s11814-017-0330-8

pISSN: 0256-1115
eISSN: 1975-7220

Fully organic CO_2 absorbent obtained by a Schiff base reaction between branched poly(ethyleneimine) and glutaraldehyde

Ki-Seob Hwang*, Hee-Young Park, Jung-Hyun Kim**, and Jun-Young Lee*,†**

*Korea Institute of Industrial Technology, 89 Yangdaegiro-gil, Ipjang-myeon, Seobuk-gu, Cheonan-si, Chungcheongnam-do 31056, Korea
**Department of Chemical Engineering, Yonsei University, 134 Shinchon-dong, Seodaemoon-gu, Seoul 03722, Korea
(*Received 21 September 2017 • accepted 23 November 2017*)

Abstract−We used a water-in-oil emulsification method to prepare particulate CO_2 absorbents from branched poly(ethyleneimine) (PEI), utilizing ^{13}C nuclear magnetic resonance spectroscopy to determine the amount of free PEI NH_2 groups and thus calculate the required cross-linker amount. The functional groups and reactivity of branched PEI particles were characterized by Fourier transform infrared spectroscopy, and their CO_2 absorption capacity was determined by thermogravimetric analysis. Dynamic light scattering measurements showed that the synthesized particles exhibited sizes of 0.2-2 μm and high surface areas, which resulted in high CO_2 absorption capacities of up to 2.18 mmol CO_2 per gram sorbent at 75 °C.

Keywords: Carbon Dioxide Absorbent, Organic Particle, Schiff Base Reaction, Primary Amine, Surface Area

INTRODUCTION

Carbon dioxide is a well-known greenhouse gas that substantially contributes to global warming along with methane [1]; the increase in atmospheric CO_2 levels (from ~270 ppm before the industrial revolution to the current value of 390 ppm) is ascribed to the increasing consumption of fossil fuels by vehicles and factories [2,3].

In the early 1990s, LiOH was suggested as an absorbent for CO_2 sequestration [4]. However, despite its high CO_2 absorption capacity of ~30 wt%, LiOH cannot be practically regenerated and separated, which precludes its use for the above purpose. Moreover, the increasing use of Li-containing compounds in industry (e.g., Li-ion batteries) has increased the global demand for Li and therefore its price.

Currently, the most promising CO_2 capturing method relies on bubbling CO_2-containing gas through an aqueous solution of amines [4], which results in the formation of carbamates and carbonates. Although these species can be conveniently decomposed to release CO_2 by changing the temperature and/or atmospheric composition, the above technology suffers from disadvantages of being area-inefficient and requiring large volumes of liquid reagents [4]; these may be offset, however, by utilizing a carbon-capture and -storage technology [4-6] based on amine beds and metal organic frameworks (MOFs) [3,7].

MOFs bind CO_2 by physical adsorption, with their adsorption capacity thus being a function of their surface area, as well as temperature and pressure [7]; high pressure is typically required for efficient CO_2 capture.

Conversely, amine beds can bind CO_2 by chemical absorption at room temperature and low pressure; as observed for MOFs, their absorption capacity increases with increasing temperature, pressure, and bed surface area. Thus, numerous researchers have attempted to surface-modify or impregnate porous materials such as silica [8-13], graphene [14], carbon nanotubes [6,15], and zeolites [7] with amines such as poly(ethyleneimine) (PEI) to increase their CO_2 capture capacity. To be practically applicable, amine beds should comprise free amine groups, have large surface areas, and exist in solid state. However, the amount of absorbed CO_2 per unit mass of PEI-impregnated porous material decreases due to the presence of the porous material. Therefore, it is necessary to study CO_2-absorbent materials using only PEI.

PEI is a typical amine polymer, with one of its variations, branched PEI (bPEI), comprising abundant primary and secondary amino groups; it thus easily reacts with CO_2 [16-20].

Herein, we prepared fully organic CO_2 absorbents by a Schiff base reaction between bPEI and glutaraldehyde (Scheme 1), and show that the thus obtained absorbent particles can be industrially applied for sequestering CO_2 generated by fossil fuel combustion.

The electrophilic aldehyde groups can be attacked by nucleophilic amines to afford imines or a Schiff bases, in which C=O bonds are replaced by C=N bonds [21,22].

As shown in Fig. 1, the size of bPEI particles prepared by Schiff

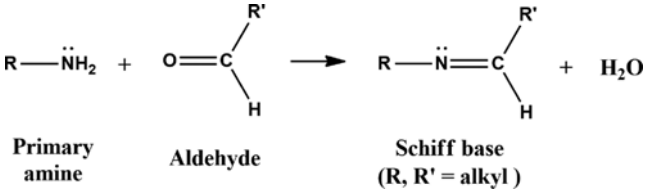

Scheme 1. A Schiff base reaction between primary amine and aldehyde.

†To whom correspondence should be addressed.
E-mail: jaylee@kitech.re.kr

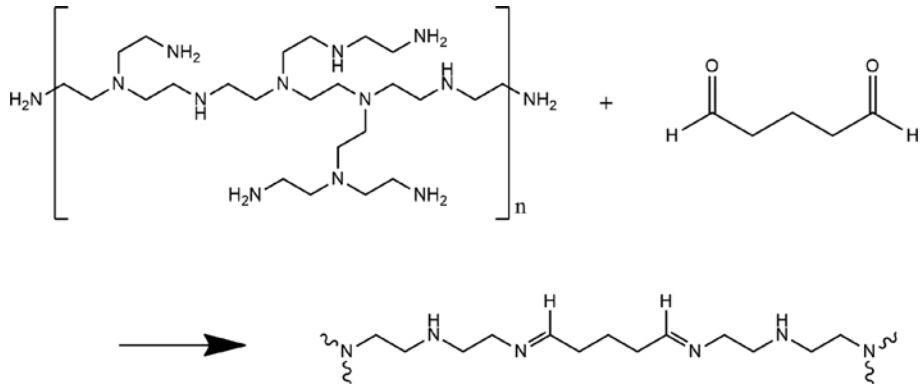

Fig. 1. The schematic of Schiff's reaction with amine of poly(ethyleneimine) and aldehyde of glutaraldehyde for CO_2 absorption organic fine particles.

base coupling has to be controlled to increase their contact area with CO_2. Therefore, these particles were prepared using an inverse emulsion method (with water as the dispersed phase and heavy mineral oil as the highly viscous continuous phase), and their CO_2 absorption capacity was determined by thermogravimetric analysis (TGA).

EXPERIMENTAL

1. Materials

The branched PEI (M_w=25 kDa) was purchased from Sigma-Aldrich (South Korea). Heavy mineral oil (density: 0.872 g·cm^{-3}) sourced from Daejung was used as the continuous phase, while deionized (DI) water (Dream Plus II, JEIO-TECH) was used as the dispersed phase. Sorbitan monooleate (Span 80, Sigma-Aldrich) was used as a surfactant and glutaraldehyde (25 wt% in water; Junsei) as a cross-linker.

2. Preparation of bPEI Particles

A 250-mL beaker was filled with mineral oil (60 g) and Span 80 (3 g), and the obtained mixture was stirred at 200 rpm for 5 min to prepare the continuous phase. A solution of bPEI in DI water (40 g at 20 wt%; dispersed phase) was added to the continuous phase and stirred for 3 min at 5,000 rpm using a homogenizer. The obtained water-in-oil emulsion was subsequently transferred to a 600-mL beaker and stirred at 200 rpm using a magnetic stirrer. The glutaraldehyde solution was introduced into the above emulsion through a 3-mm-diameter latex tube at a flow rate of 0.2 mL·min^{-1} using a dispenser (UniSpense PRO, Wheaton), and the cross-linking reaction was allowed to proceed for 24 h at 25 °C (Table 1). According to the amount of added glutaraldehyde relative to the necessary amount of theoretical cross-linking with the primary amines of branched PEI, we named the synthesized particles as cPEI-GA 18, cPEI-GA 24, and cPEI-GA 36, as shown in Table 1. The treated emulsion was co-centrifuged with isopropyl alcohol three or four times to remove the mineral oil and unreacted bPEI; the solid residue was dried in a vacuum oven for 12 h. The amount of glutaraldehyde was chosen based on the number of amino groups determined by ^{13}C nuclear magnetic resonance (NMR).

3. Quantitation of Amino Groups

The number of primary amino groups on bPEI and thus the required amount of the cross-linking agent were determined by ^{13}C NMR (Bruker Avance III) analysis of 1 wt% bPEI solutions in D_2O containing 0.05 wt% tetramethylsilane as the internal standard.

The number of primary and secondary amine groups on bPEI significantly affects its CO_2 absorption capacity. If the amount of utilized glutaraldehyde exceeds that necessary for cross-linking bPEI molecules, the amount of amine groups capable of reacting with CO_2 decreases due to excessive formation of imino moieties. If an insufficient amount of glutaraldehyde is used, on the other hand, the produced particles are unstable and transform into a gel due to the absorption of water and resultant swelling. Therefore, the determination of optimal glutaraldehyde loading was of great importance.

To achieve this, bPEI was characterized by inverted-gate ^{13}C NMR, and the signals in each spectrum were assigned according to literature [16]. Based on the integrated signals of carbons adjacent to primary, secondary, and tertiary amino groups, the ratio of these groups could be calculated using the following formula:

$$NH_2 : NH : N = I(C_{1\text{-}2}+C_{1\text{-}3}) : I(C_{2\text{-}1}+C_{2\text{-}2}+C_{2\text{-}3})/2 : I(C_{3\text{-}1}+C_{3\text{-}2}+C_{3\text{-}3})/3 \quad (1)$$

where $NH_2 : NH : N$ is the ratio of primary, secondary, and tertiary amino groups; $I(C_{1\text{-}2}+C_{1\text{-}3})$ is the integrated signal of carbons adjacent to primary amino groups; $I(C_{2\text{-}1}+C_{2\text{-}2}+C_{2\text{-}3})$ is the integrated signal of carbons adjacent to secondary amino groups; and $I(C_{3\text{-}1}+$

Table 1. The amount of glutaraldehyde for cross-linking reaction between primary amine of branched PEI using Schiff's base reaction

Sample	Branched PEI (g)	Glutaraldehyde (g)	Mole of glutaraldehyde (mmol)	(Amount of added glutaraldehyde)/(Necessary amount of theoretical cross-linking reaction between primary amine)
cPEI-GA18	8.0	0.62	6.2	0.18
cPEI-GA27		0.93	9.3	0.27
cPEI-GA36		1.23	12.3	0.36

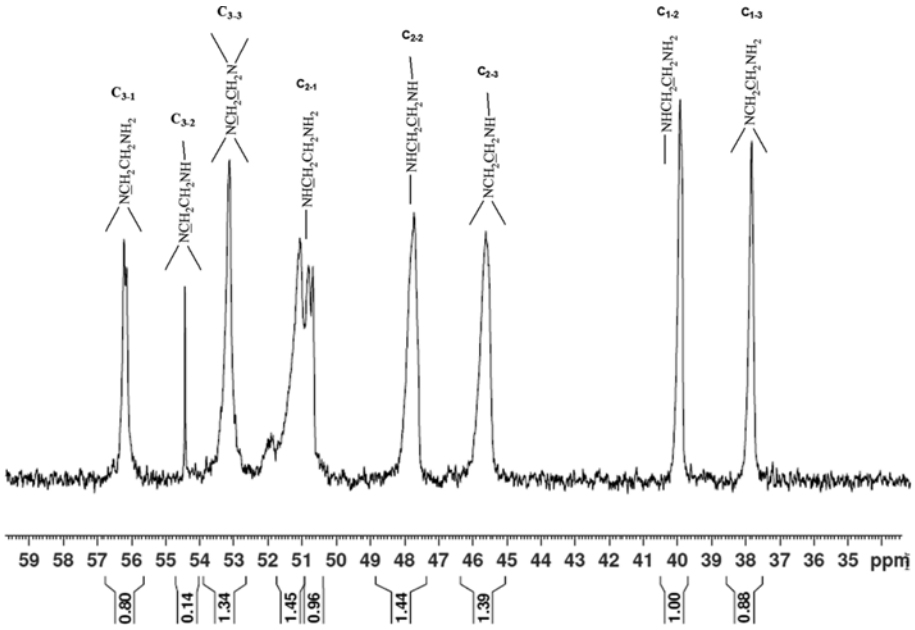

Fig. 2. ^{13}C NMR spectrum of branched PEI (25K Dalton) to find out the number of primary amine groups on branched PEI.

C_{3-2}+C_{3-3}) is the integrated signal of carbons adjacent to tertiary amino groups [20,22]. The primary, secondary, and tertiary amino groups had relative abundances of 37.8, 38.1, and 24.1%, respectively, as shown in Fig. 2. Additionally, the utilized bPEI was demonstrated to have a branching degree of 0.61 and possess an average of 569 free amino groups per molecule. Thus, 8 g of bPEI contained 68.9 mmol of primary amino groups [23].

4. Characterization of Cross-linked PEI (cPEI) Particles

Spectroscopy measurements using ^{13}C cross-polarization/magic angle spinning nuclear magnetic resonance (CP/MAS ^{13}C NMR) were performed on a high-resolution 400-MHz Bruker solid-state Fourier transform-NMR (FT-NMR) spectrometer using a conventional method. The rotor containing PEI particles was spun at 3.5 kHz, and the 90° pulse duration, contact time, and repetition time equaled 4 μs, 2 ms, and 3 s, respectively. For each spectrum, 4096 scans were recorded, and the ^{13}C chemical shifts were calibrated using the carbonyl carbon resonance of glycine as an external reference at 176.03 ppm. Fourier transform infrared (FT-IR) spectra were recorded on a Varian 660-IR instrument in attenuated total reflection mode in the range of 4,000-400 cm^{-1}. PEI particle size

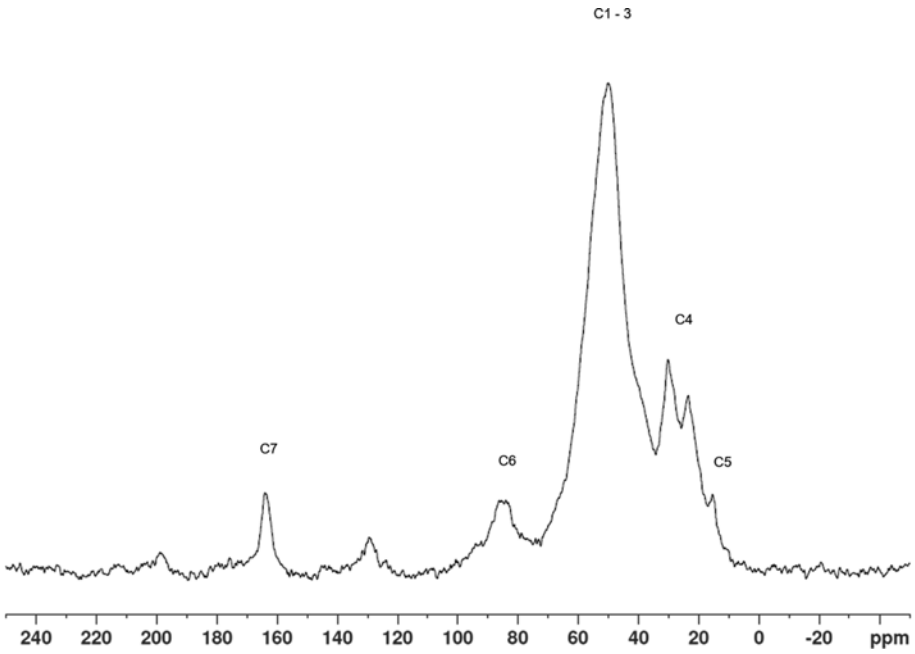

Fig. 3. CP/MAS solid state ^{13}C NMR spectrum of cPEI-GA36 organic fine particles to confirm Schiff's reaction.

distributions were determined by dynamic light scattering (DLS; Mastersizer 2000, Malvern) using isopropanol as a dispersant. Field emission scanning electron microscopy (FE-SEM) imaging of Pt-coated samples was conducted using a JEOL JSM-6701F instrument. The thermal stability of the cPEI particles was probed by TGA (Q500, TA Instruments) in an atmosphere of N_2 at temperatures between 100 and 600 °C. CO_2 absorption capacity was determined from mass changes upon CO_2 exposure at 75 °C. Briefly, CO_2 absorption was performed by exposing samples (purged with N_2 to achieve a constant mass) to a flow of CO_2 gas for 200 min, with CO_2 desorption conducted by 180-min purging with N_2 gas. The above adsorption and desorption was counted as one cycle, with two cycles utilized in this study.

RESULTS AND DISCUSSION

The molecular structures of PEI particles before and after surface treatment were probed by ^{13}C CP/MAS NMR (Fig. 3); the signal at 49.9 ppm was ascribed to carbon atoms in the main chain of bPEI [24], while peaks at 30.1, 23.4, and 15.3 ppm were attributed to aliphatic C=N and methyl carbons [25]. The peak at 85.4 ppm corresponded to -CH_2N groups, and that at 164.0 ppm represented imine groups [26] produced during the Schiff base reaction. The peaks at 198.8 and 131.6 ppm were assigned to the side beds of the imine groups. Thus, ^{13}C CP/MAS NMR analysis showed that the Schiff base reaction proceeded successfully.

Peaks observed in the FT-IR spectrum of bPEI (Fig. 4) at 3,357-3,295 cm^{-1} corresponded to the N-H stretch of primary and secondary amines, with two peaks signifying primary amines and a single peak signifying secondary amines [24]. Bands at 2,935 and 2,813 cm^{-1} indicated symmetrical and asymmetrical C-H stretches, respectively, and signals in the range of 1,560-1,640 cm^{-1} corresponded to N-H bending vibrations of primary and secondary amines. The peak at 1,465 cm^{-1} was ascribed to C-H bending, and those at 1,000-1,350 cm^{-1} corresponded to C-N stretching [27-29], which had previously been observed for cPEI particles.

Comparison of the cPEI and bPEI spectra revealed that the former contained a peak at 1,656 cm^{-1} that was not present in the latter; this peak consequently was ascribed to C=N stretching. As the amount of crosslinking agent increased, the peak at 3,357 cm^{-1} as amines (primary amines) chemically shifted to a single peak at 3,400 cm^{-1} corresponding to unsubstituted amides (-(=)N^+H); this indicates that the primary amines reacted with glutaraldehyde [30].

Fig. 5 shows that cPEI particles exhibited sizes of 0.2-2 μm. Fig. 6 shows FE-SEM images of cPEI particles produced using differ-

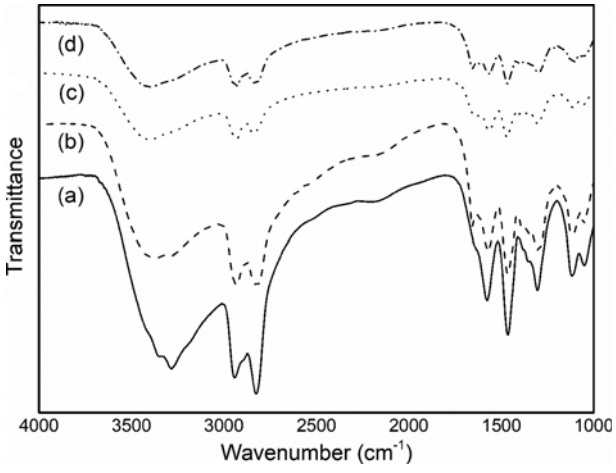

Fig. 4. FT-IR spectra of branched PEI (a), cPEI-GA18 (b), cPEI-GA27 (b), and cPEI-GA36 (d) to check peaks of amine and Schiff's reaction.

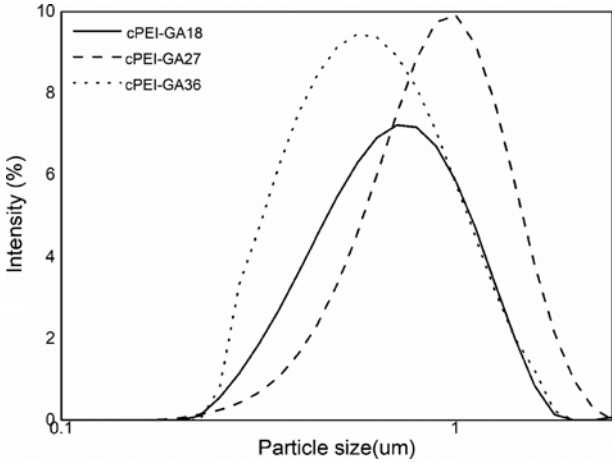

Fig. 5. The particle size distributions of cross-linked PEI organic fine particles according to added amount of glutaraldehyde.

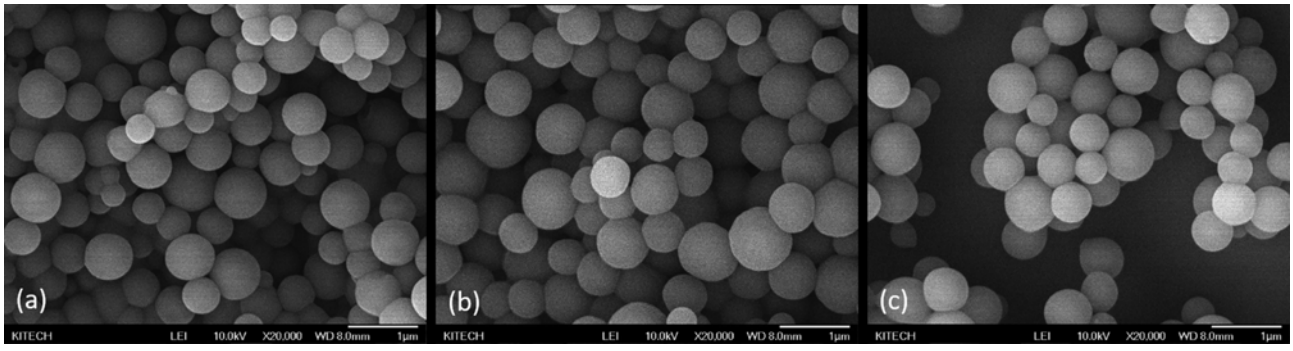

Fig. 6. FE-SEM images of cross-linked PEI organic fine particles to confirm the morphology and particle size. (a) cPEI-GA18, (b) cPEI-GA27, and (c) cPEI-GA36.

Table 2. Specific surface area of cross-linked PEI organic fine particles

PEI Mw.	Sample name	Specific surface area (m^2/g)
25,000	cPEI-GA18	6.66
	cPEI-GA27	6.92
	cPEI-GA36	10.20

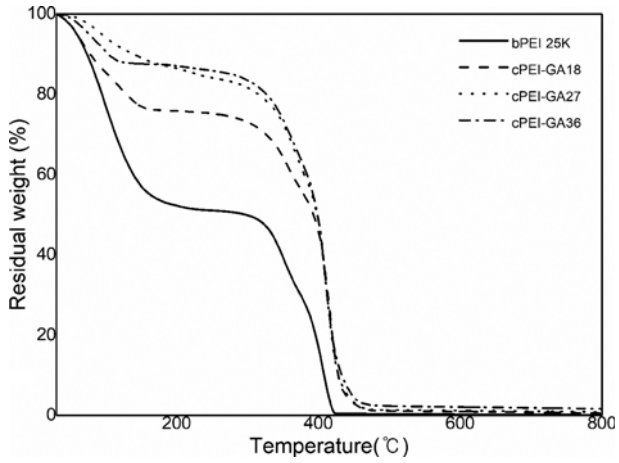

Fig. 7. Thermal stabilities of branched PEI and cross-linked PEI organic fine particles using thermogravimetric analysis curves.

ent glutaraldehyde amounts, demonstrating that these particles had not aggregated and exhibited spherical shapes.

Cross-linking of bPEI in aqueous solutions results in the formation of a network structure, which is translated into a certain specific surface area. Likewise, particles prepared by cross-linking in an inverse emulsion also form a network structure, which features external and internal micropores; it should thus be capable of expansion and contraction to some extent. As the amount of the cross-linking agent was increased, the cross-linking density increased and the particle size decreased, while the specific surface area increased. The specific surface area value is shown in Table 2.

Since the thermal stability of the cPEI particles largely determines the scope of their potential applications, we characterized bPEI and cPEI particles by TGA to compare their thermal behaviors and to correlate their thermal stabilities to the extent of cross-linking (Fig. 7).

The mass loss observed for bPEI between ~30 and 160 °C was ascribed to desorption of physically adsorbed CO_2 and water evaporation [31]. A gradual mass loss was subsequently observed up to 250 °C, becoming much more pronounced at 300-400 °C, with complete decomposition observed at ~420 °C. Similarly, the mass

Table 3. CO_2 adsorption comparison of cross-linked PEI organic fine particles

Sample name	CO_2 adsorption Max. (mg CO_2/g sorbent)	CO_2 adsorption Max. (mmol CO_2/g-sorbent)
cPEI-GA18	72.31	1.64
cPEI-GA27	90.02	2.05
cPEI-GA36	95.80	2.18

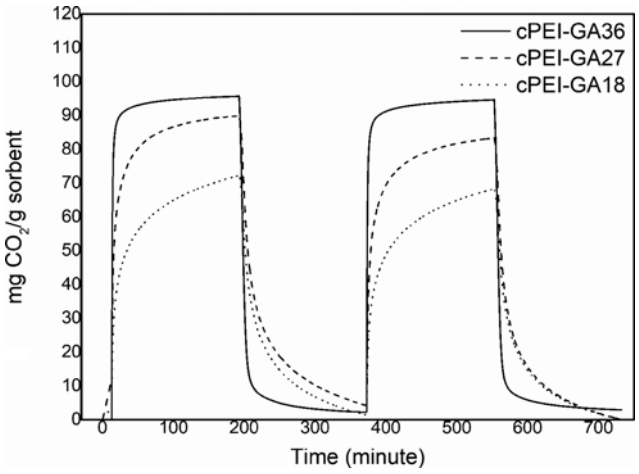

Fig. 8. The measurement of CO_2 absorption and desorption properties of cross-linked PEI organic particles with exchanged purging gases with CO_2 and N_2 on each 200 minutes.

loss observed for cPEI particles at 50-160 °C was ascribed to CO_2 and water loss, and the significant mass loss observed above 300 °C was similar to that of bPEI but more gradual, with 80% of cPEI particles remaining intact even at ~350 °C. For cPEI, the final decomposition temperature equaled 450 °C, which was ~50 °C higher than for bPEI. This was due to the increased thermal stability provided by the cross-linking procedure. Thus, cPEI was demonstrated to be more thermally stable than bPEI, exhibiting an extended range of potential applications.

The reaction of PEI amino groups with atmospheric CO_2 to afford ammonium carbamates (Scheme 2) is known to be affected by temperature and atmospheric composition. In addition, under constant pressure conditions CO_2 can be desorbed by increasing the absorbent temperature or nitrogen gas content.

We characterized the CO_2 absorption performance of each produced cPEI sample. For maximum CO_2 desorption, samples were purged with nitrogen for 200 min at 75 °C, which corresponds to the optimum CO_2 adsorption/desorption temperature. Subsequently,

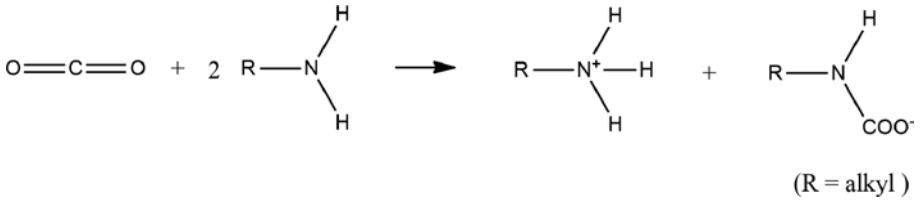

Scheme 2. The reaction of primary amine with CO_2 to afford alkyl ammonium ion and alkyl carbamate ion.

samples were exposed to CO_2 for 180 min to determine their maximum specific absorption capacities (Table 3). Fig. 8 shows the dependence of the absorbed CO_2 amount on the exposure time, revealing that more than 90% of CO_2 could be absorbed within 30 min. Among the produced samples, cPEI-GA36 (shown in Table 1) exhibited the highest CO_2 absorption capacity (2.18 $mmol \cdot g^{-1}$) due to having a high molecular weight and thus a greater amount of secondary amino groups and largest surface area. The reason that CO_2 absorption and desorption in cPEI-GA36 was faster than for the other samples, was that cPEI-GA36 had many primary amines on the surfaces of the particles, which had the smallest average size and largest surface area.

The absorbent prepared here did not comprise inorganic particles such as SiO_2, but rather relied on an adequate extent of cross-linking to establish optimal CO_2 adsorption characteristics. The 100% organic absorbent here had a lower density than sorbents containing inorganic particles, thus featuring a larger amount of amino groups per unit weight. However, even though the above absorbent was expected to exhibit a high CO_2 absorption capacity, the observed values were similar to those of its porous counterparts, which can be ascribed to the low specific surface area (5 $m^2 \cdot g^{-1}$) of cPEI. However, for porous composite absorbents, excessive impregnation (>50%) is known to decrease the CO_2 absorption capacity due to a decrease in specific surface area. Therefore, by controlling the specific surface area of cPEI, we achieved an increase in its specific CO_2 absorption capacity.

CONCLUSION

We successfully prepared a high-performance CO_2 absorbent by cross-linking the amine groups of branched poly(ethyleneimine) (bPEI) with glutaraldehyde using an inverse emulsion technique. To determine the optimal amount of the cross-linking agent, the number of primary amino groups was quantified by ^{13}C nuclear magnetic resonance (NMR) analysis. As a result, glutaraldehyde loadings of 7.8, 11.6, and 15.4% were used (100%=complete cross-linking of all primary amino groups), yielding crosslinked PEI (cPEI) particles with sizes of 0.2-5 μm and a maximum specific surface area of only 10.20 $m^2 \cdot g^{-1}$. The maximum CO_2 absorption capacity of 2.18 $mmol \cdot g^{-1}$ sorbent was observed for cPEI-GA36. Although the exclusion of inorganic matter was expected to increase the specific CO_2 absorption capacity, the small specific surface area of the fabricated absorbent resulted in CO_2 being absorbed only on its surface, resulting in a performance similar to that of impregnated materials. Therefore, specific surface area control may allow the production of particles with enhanced CO_2 absorption capacities. Although the CO_2 absorption properties of the absorbent prepared here were not compared with those of variable-surface-area liquid PEI, the former outperformed other solid absorbents that were previously reported. Liquid PEI is of limited practical applicability, whereas solid absorbents find numerous applications in various fields. Thus, the developed dry sorbent here may be expected to make up for the known disadvantages of organic/inorganic hybrids, such as complex fabrication processes and PEI elution from the absorbent, while the manufacture of nanometer-sized globular particles selectively absorbing CO_2 can potentially be applied in various areas such as polymer composites and fillers.

ACKNOWLEDGEMENTS

This work was supported by Korea Institute of Planning and Evaluation for Technology in Food, Agriculture, Forestry (IPET) through Technology Commercialization Support Program, funded by Ministry of Agriculture, Food and Rural Affair (MAFRA) (815002).

REFERENCES

1. J. Wang, H. Chen, H. Zhou, X. Liu, W. Qiao, D. Long and L. Ling, *J. Environ. Sci.*, **25**, 124 (2013).
2. H. Yang, Z. Xu, M. Fan, R. Gupta, R. B. Slimane, A. E. Bland and I. Wright, *J. Environ. Sci.*, **20**, 14 (2008).
3. Y. Lin, Q. Yan, C. Kong and L. Chen, *Sci. Rep.*, **3**, 1859 (2013).
4. S. Satyapal, T. Filburn, J. Trela and J. Strange, *Energy Fuels*, **15**, 250 (2001).
5. J. Liu, Y. Liu, Z. Wu, X. Chen, H. Wang and X. Weng, *J. Colloid Interface Sci.*, **386**, 392 (2012).
6. E. P. Dilllon, C. A. Crouse and A. R. Barron, *ACS Nano*, **2**, 156 (2008).
7. B. Arstad, H. Fjellvåg, K. O. Kongshaug, O. Swang and R. Blom, *Adsorption*, **14**, 755 (2008).
8. R. Sanz, G. Calleja, A. Arencibia and E. S. Sanz-Pérez, *Appl. Surf. Sci.*, **256**, 5323 (2010).
9. W.-J. Son, J.-S. Choi and W.-S. Ahn, *Micropor. Mesopor. Mater.*, **113**, 31 (2008).
10. T. Zhu, S. Yang, D. K. Choi and K. H. Row, *Korean J. Chem. Eng.*, **27**, 1910 (2010).
11. Y. Liu, Q. Ye, M. Shen, J. Shi, J. Chen, H. Pan and Y. Shi, *Environ. Sci. Technol.*, **45**, 5710 (2011).
12. P. Kumar, S. Kim, J. Ida and V. V. Guliants, *Ind. Eng. Chem. Res.*, **47**, 201 (2008).
13. J. C. Hicks, J. H. Drese, D. J. Fauth, M. L. Gray, G. Qi and C. W. Jones, *J. Am. Chem. Soc.*, **130**, 2902 (2008).
14. S. Yang, L. Zhan, X. Xu, Y. Wang, L. Ling and X. Feng, *Adv. Mater.*, **25**, 2130 (2013).
15. M.-S. Lee, S.-Y. Lee and S.-J. Park, *Int. J. Hydrogen Energy*, **40**, 3415 (2015).
16. H. Liu, Z. Shen, S.-E. Stiriba, Y. Chen, W. Zhang and L. Wei, *J. Polym. Sci. Part A: Polym. Chem.*, **44**, 4165 (2006).
17. M. R. Park, K. O. Han, I. K. Han, M. H. Cho, J. W. Nah, Y. J. Choi and C. S. Cho, *J. Control Release.*, **105**, 367 (2005).
18. H. Petersen, P. M. Fechner, D. Ficher and T. Kissel, *Macromolecules*, **35**, 6867 (2002).
19. L. Y. Qiu and Y. H. Bae, *Biomaterials*, **28**, 4132 (2007).
20. H. Pertersen, T. Merdan, K. Kunath, D. Fucher and T. Kissel, *Bioconjugate Chemistry*, **13**, 812 (2002).
21. H. R. Allcock and P. E. Austin, *Macromolecules*, **41**, 1616 (1981).
22. M. Kramer, J. F. Stumbe, G. Grimm, B. Kaufmann, U. Kruger, M. Weber and R. Haag, *Chembiochem.*, **5**, 1081 (2004).
23. K. Kunath, *J. Controlled Release*, **89**, 113 (2003).
24. B. Xia, C. Dong, Y. Lu, M. Rong, Y.-z. Lv and J. Shi, *Thin Solid Films*, **520**, 1120 (2011).

25. M. K. Bhunia, S. K. Das, P. Pachfule, R. Banerjee and A. Bhaumik, *Dalton Trans.*, **41**, 1304 (2012).
26. A. V. Pestov, A. V. Mehaev, M. I. Kodess, M. A. Ezhikova, Y. A. Azarova and S. Y. Bratskaya, *Carbohydr. Polym.*, **138**, 252 (2016).
27. M. D. Rubianes and M. C. Strumia, *Electroanalysis*, **22**, 1200 (2010).
28. H. V. Adikane and G. J. Iyer, *Appl. Biochem. Biotechnol.*, **169**, 1026 (2013).
29. A. Wnorowski and V. A. Yaylayan, *J. Agricult. Food Chemistry*, **51**, 6537 (2003).
30. M. M. M. Elnashar, M. A. Yassin and T. Kahil, *J. Appl. Polym. Sci.*, **109**, 4105 (2008).
31. F. Wang, P. Liu, T. Nie, H. Wei and Z. Cui, *Int. J. Mol. Sci.*, **14**, 17 (2012).